CrystEngComm

Accepted Manuscript

This article can be cited before page numbers have been issued, to do this please use: P. S. Hariharan, D. Moon and P. P. Anthony, *CrystEngComm*, 2017, DOI: 10.1039/C7CE01650F.

ROYAL SOCIETY OF CHEMISTRY

rsc.li/crystengcomm

View Article Online
DOI: 10.1039/C7CE01650F

Journal Name

ARTICLE

Crystallization induced reversible fluorescence switching and alkyl chain length dependent thermally stable supercooled organic fluorescent liquid

Received 00th January 20xx,
Accepted 00th January 20xx

DOI: 10.1039/x0xx00000x

www.rsc.org/

P. S. Hariharan,[a] Dohyun Moon*[b] and Savarimuthu Philip Anthony*[a]

Highly stable supercooled fluorescent liquid and crystallization induced reversible fluorescence switching has been achieved via varying alkyl chain length of alkoxy group in triphenylamine aldehyde, (4-(diphenylamino)-methoxybenzaldehyde (DPAMB). DPAMB and different alkyl chain, ethyl (DPAEB), propyl (DPAPrB), butyl (DPABB), pentyl (DPAPeB), hexyl (DPAHB) and cyanohexyl (DPAH-CNB) substituted compound exhibited weak fluorescence (λ_{max} between 429 and 490 nm) in the solid state except DPAEB that did not show any measurable fluorescence. Structural analysis were performed to get the insight of alkyl chain length effect on the molecular packing in the solid state. The strong crushing of all solids lead to drastic enhancement of fluorescence intensity without altering λ_{max}. Interestingly, the melt of all compounds showed strong fluorescence with red shift of fluorescence λ_{max} (460 – 489 nm). Slight rubbing of the melts exhibited reversible fluorescence switching. Powder X-ray diffraction (PXRD) studies suggested the conversion of crystalline to amorphous and vice versa while melting of solids and rubbing of melt was responsible fluorescence switching. Importantly, the melt showed alkyl chain length dependent stable supercooled fluorescent liquid at room temperature. Differentail scanning caolorimetry (DSC) indicated crystallization of melt while heating/cooling of DPAMB and DPAEB melt whereas DPAPrB, DPABB, DPAPeB, DPAHB and DPAH-CNB did not show any crystallization in the subsequent cooling/heating cycles. Thus alkyl chain length and propeller molecular shape of triphenylamine has been utilized for developing strongly fluorescent supercooled fluorescent liquid at room temperature.

Introduction

Switchable and tunable organic solid state fluorescent materials have received considerable interest in recent years because of their potential applications in optoelectronics, optical recording, security inks and fluorescent sensors.[1] However, molecular conformation, packing and intermolecular interactions significantly influences on the solid state fluorescent properties especially tuning and switching of fluorescence. Subtle conformational and/or molecular packing modulation of fluorophore often resulted in tunable solid state fluorescence materials.[2] Organic molecular structures and the resultant materials that exhibit conformational and phase change while applying external stimuli such as shear, light, solvent vapor and heat produced switchable fluorescent materials.[3] For example, organic solid state fluorescent materials constructed using non-planar propeller core often produced stimuli responsive reversible and self-reversible fluorescence switching smart materials due to planarization of core and phase change.[4] Temperature controlled molecular packing in a excited state intramolecular proton transfer (ESIPT) and terpyridine compound lead to reversible fluorescence switching.[5] Halochromic functionalities in organic fluorescent materials have also been exploited to demonstrate tunable and switchable fluorescence as well as optical data recording and storage applications.[6]

Alkyl groups have been successfully utilized to improve the solubility of π–conjugated organic molecules for fabricating electronic and opto-electronic devices. Although, alkyl chain length hardly affect the fluorescent properties in the solution state, it strongly influences on the molecular conformations and packing in the solid state, thus their optical and opto-electronic properties.[7] Alkyl chain length have been successfully employed to develop several class of external stimuli responsive mechanofluorochromic materials.[8] Flexible alkoxy-alkyl substitution in diaminodicyanoquinodimethane based donor-acceptor produced extensive mechanofluorochromism through reversible transformation of crystalline to amorphous phase.[9] Diphenylfluorenone derivatives showed multi-stimuli induced reversible fluorescence switching dependent on the alkyl chain length and position of substitution.[10] However, utilization of alkyl chain length for fabricating supercooled fluorescent liquid and crystallization induced reversible fluorescence switching materials are rarely demonstrated.[11]

Herein, we report the synthesis of crystallization induced reversible fluorescence switching and stable supercooled fluorescent liquid compounds based on triphenylamine

[a] Department of Chemistry, School of Chemical & Biotechnology, SASTRA University, Thanjavur-613401, Tamil Nadu, India. E-mail: philip@biotech.sastra.edu
[b] Beamline Department, Pohang Accelerator Laboratory, 80 Jigokro-127beongil, Nam-gu, Pohang, Gyeongbuk, Korea. E-mail: dmoon@postech.ac.kr
[c] Electronic Supplementary Information (ESI) available: [Synthesis, NMR data, absorption spectra, crystal structures, PXRD pattern. See DOI: 10.1039/x0xx00000x

View Article Online
DOI: 10.1039/C7CE01650F

aldehyde, (4-(diphenylamino)-methoxybenzaldehyde (DPAMB) through changing alkyl chain length in the alkoxy position. The powders of DPAMB and different alkyl chain, ethyl (DPAEB), propyl (DPAPrB), butyl (DPABB), pentyl (DPAPeB), hexyl (DPAHB) and cyanohexyl (DPAH-CNB) substituted compounds exhibited weak blue fluorescence (λ_{max} between 429 and 490 nm) except DPAEB that did not show any measurable fluorescence. Interestingly melting of all compounds lead to strong enhancement of fluorescence intensity with red shift of fluorescence peak (λ_{max} = 460 – 489 nm). The melts exhibited chain length dependent crystallization upon cooling and blue shift of fluorescence. DPAMB and DPAEB showed immediate crystallization and fluorescence switching whereas higher alkyl chain substituted compounds showed stable melts. Importantly, DPAPeB, DPAHB and DPAH-CNB compounds are stable as supercooled fluorescent liquid without crystallization. However, slight rubbing of the melts exhibited immediate crystallization followed by blue shift of fluorescence. DSC studies further support that triphenylamine (TPA) compounds with higher alkyl chain did not show crystallization upon cooling/heating as well as re-melting upon second heating. Single crystal structural analysis revealed that alkyl chain influenced on the conformation of TPA and higher alkyl chain length lead to the assembly of lamellar structure in the crystal lattice. PXRD studies suggested reversible conversion crystalline to amorphous phase and vice versa upon melting and rubbing.

Experimental Section

Dimethylformamide (DMF, HPLC grade), phosphorous oxychloride, triphenylamine, 3-methoxy-N,N-diphenylaniline, alkyl bromides were purchased from Sigma-Aldrich and used without further purification. Acetonitrile, ethanol, methanol, hexane and dichloromethane solvents were purchased from Merck India and used without further purification.

General procedure for introducing aldehyde functionality

Aldehyde functionality was introduced following a reported Vilsmeier–Haack formylation procedure (Scheme S1).[12] In a typical procedure, phosphorous oxychloride (1.1 mL, 12 mmol) was added drop-wise into DMF (2 mL, 24 mmol) at 0 °C (cooled in ice-salt mixture) and the reaction mixture was stirred for 45 minutes. Then, triphenylamine/3-methoxy-N,N-diphenylaniline (4 mmol) was added slowly. The reaction mixture was brought to room temperature and stirred at 60°C for 2 h. After cooling, the reaction mixture was poured into ice-water (200 mL) and neutralized using 1.0 M NaOH. The product was extracted using CH_2Cl_2. The combined extract was washed with water and brine solution and dried over Na_2SO_4. The solvent was evaporated and purified using column chromatography (ethyl acetate:hexane (1:10)).

4-(diphenylamino)benzaldehyde (DPAB)

Single crystals were grown from ethanol at room temperature. Yield: 85%. M. p.: 134° C, ^1H-NMR (400 MHz, $CDCl_3$) δ 9.81 (s, 1H), 7.70-7.66 (m, 2H), 7.38-7.31 (m, 4H), 7.19-7.14 (m, 6H), 7.04-6.99 (m, 2H). ^{13}C-NMR (125 MHz, $CDCl_3$) δ 190.46, 153.37, 146.16, 131.32, 129.74, 129.10, 126.33, 125.12, 119.35. $C_{19}H_{15}NO$ (273.33): calcd. C 83.49, H 5.53, N 5.12; found C 83.72, H 5.36, N 5.42.

4-(diphenylamino)-2-methoxybenzaldehyde (DPAMB)

Single crystals were grown from ethanol at room temperature. Yield: 80%. M. p.: 134° C, ^1H-NMR (400 MHz, $CDCl_3$) δ 10.22 (s, 1H), 7.66 (d, 1H), 7.37-7.31 (m, 4H), 7.20-7.14 (m, 6H), 6.54-6.51 (m, 1H), 6.45 (d, 1H), 3.690 (s, 3H). ^{13}C-NMR (125 MHz, $CDCl_3$) δ 187.85, 163.12, 154.87, 146.10, 129.91, 129.67, 126.47, 125.17, 118.21, 112.23, 101.73, 55.41. $C_{20}H_{17}NO_2$ (303.35): calcd. C 79.19, H 5.65, N 4.62; found C 79.22, H 4.56, N 4.52.

General procedure for the preparation of 4-(diphenylamino)-2-alkoxy benzaldehyde

4-(diphenylamino)-2-hydroxybenzaldehyde was synthesized by converting OCH_3 group of DPAMB to OH by stirring with BBr_3 in CH_2Cl_2 following the reported procedure (Scheme S1).[13] To the stirred solution of 4-(diphenylamino)-2-hydroxybenzaldehyde (1.0 equivalent) in DMSO, alkyl bromides (ethyl, propyl, butyl, pentyl, hexyl and cyanohexyl bromide, 1.3 equivalents) and potassium carbonate (5.0 equivalents) were added and the reaction mixture was stirred at 100° C for 6 h. After completion of the reaction (reaction progress was monitored by TLC), the reaction mixture was brought to room temperature and added into ice-cold water. The product was extracted with CH_2Cl_2 for several times and combined CH_2Cl_2 was washed using brine solution and dried over Na_2SO_4. The solvent was evaporated and the product was purified using column chromatography (ethyl acetate - hexane mixture (1:10)). The white/light yellow colored viscous liquid product was slowly solidified upon storing in refrigerator.

4-(diphenylamino)-2-ethoxybenzaldehyde (DPAEB)

Single crystals were grown from ethanol by storing at 4 °C for 4 days. Yield: 75%. M. p: 111 °C, ^1H-NMR (400 MHz, $CDCl_3$) δ 10.27 (s, 1H), 7.66 (d, 1H), 7.36-7.31 (m, 4H), 7.19-7.14 (m, 6H), 6.53-6.50 (m, 1H), 6.43 (d, 1H), 3.91-3.84 (q, 2H), 1.39-1.34 (t, 3H). ^{13}C-NMR (125 MHz, CDCl3) δ 187.98, 162.60, 154.77, 146.14, 129.61, 129.45, 126.38, 125.04, 118.29, 112.28, 102.68, 63.86, 14.45. $C_{21}H_{19}NO_2$ (317.38): calcd. C 79.47, H 6.03, N 4.41; found C 78.92, H 6.46, N 4.22.

4-(diphenylamino)-2-propoxybenzaldehyde (DPAPrB)

Single crystals were grown from ethanol by storing at 4 °C for 4 days. Yield: 78%. M. p: 100 °C, ^1H-NMR (400 MHz, $CDCl_3$) δ 10.29 (s, 1H), 7.66 (d, 1H), 7.38-7.31 (m, 4H), 7.19-7.14 (m, 6H), 6.53-6.49 (m, 1H), 6.43 (d, 1H), 3.79-3.75 (t, 2H), 1.82-1.71 (m, 2H), 1.02-0.97 (t, 3H). ^{13}C-NMR (125 MHz, CDCl3) δ 187.92, 162.84, 154.81, 146.16, 129.64, 129.39, 126.40, 125.07, 118.38, 112.30, 102.69, 69.65, 22.34, 10.55. $C_{22}H_{21}NO_2$ (331.41): calcd. C 79.73, H 6.39, N 4.23; found C 79.86, H 6.30, N 4.52.

4-(diphenylamino)-2-butoxy-benzaldehyde (DPABB)

Single crystals were grown from hexane by storing at 4 °C for 7 days. Yield: 80%. M. p: 84° C, ^1H-NMR (400 MHz, $CDCl_3$) δ 10.27 (s, 1H), 7.66 (d, 1H), 7.37-7.31 (m, 4H), 7.19-7.14 (m, 6H), 6.53-6.49 (m, 1H), 6.43 (d, 1H), 3.83-3.79 (t, 2H), 1.76-1.67 (m, 2H), 1.51-1.38 (m, 2H), 0.96-0.91 (t, 3H). ^{13}C-NMR (125 MHz, $CDCl_3$)

View Article Online
DOI: 10.1039/C7CE01650F

δ 187.94, 162.83, 154.81, 146.16, 129.64, 129.38, 126.41, 125.07, 118.37, 112.28, 102.67, 67.89, 30.97, 19.23, 13.80. $C_{23}H_{23}NO_2$ (345.43): calcd. C 79.97, H 6.71, N 4.05; found C 80.12, H 6.86, N 4.10.

4-(diphenylamino)-2-(pentyloxy)benzaldehyde (DPAPeB)

Single crystals were grown from hexane by storing at 4 °C for 7 days. Yield: 82%. M. p.: 96° C, ^1H-NMR (400 MHz, $CDCl_3$) δ 10.27 (s, 1H), 7.66 (d, 1H), 7.37-7.31 (m, 4H), 7.19-7.14 (m, 6H), 6.53-6.49 (m, 1H), 6.43 (d, 1H), 3.82-3.78 (t, 2H), 1.78-1.59 (m, 2H), 1.44-1.27 (m, 4H), 0.93-0.88 (t, 3H). ^{13}C-NMR (125 MHz, $CDCl_3$) δ 187.96, 162.84, 154.81, 146.16, 129.64, 129.37, 126.40, 125.07, 118.36, 112.28, 102.66, 68.20, 28.63, 28.19, 22.39, 14.00. $C_{24}H_{25}NO_2$ (359.46): calcd. C 80.19, H 7.01, N 3.90; found C 80.44, H 6.86, N 4.12.

4-(diphenylamino)-2-(hexyloxy)benzaldehyde (DPAHB)

Single crystals were grown from hexane by storing at 4 °C for 7 days. Yield: 78%. M. p.: 77° C, ^1H-NMR (400 MHz, $CDCl_3$) δ 10.27 (s, 1H), 7.66 (d, 1H), 7.37-7.31 (m, 4H), 7.19-7.14 (m, 6H), 6.53-6.49 (m, 1H), 6.43 (d, 1H), 3.82-3.78 (t, 2H), 1.77-1.68 (m, 2H), 1.45-1.34 (m, 2H), 1.32-1.25 (m, 4H), 0.91-0.87 (t, 3H). ^{13}C-NMR (125 MHz, $CDCl_3$) δ 187.94, 162.84, 154.81, 146.17, 129.63, 129.37, 126.40, 125.06, 118.38, 112.29, 102.69, 68.22, 31.49, 28.90, 25.68, 22.54, 14.00. $C_{25}H_{27}NO_2$ (373.49): calcd. C 80.40, H 7.29, N 3.75; found C 80.72, H 7.38, N 3.63.

6-(5-(diphenylamino)-2-formylphenoxy)hexanenitrile (DPAH-CNB)

Single crystals were grown from hexane by storing at 4 °C for 7 days. Yield: 80%. M. p.: 89° C, ^1H-NMR (400 MHz, $CDCl_3$) δ 10.24 (s, 1H), 7.66 (d, 1H), 7.37-7.31 (m, 4H), 7.20-7.15 (m, 6H), 6.55-6.51 (m, 1H), 6.41 (d, 1H), 3.84-3.80 (t, 2H), 2.39-2.35 (t, 3H). ^{13}C-NMR (125 MHz, $CDCl_3$) δ 187.61, 162.47, 154.86, 146.06, 129.69, 126.46, 125.21, 119.49, 118.20, 112.34, 102.40, 67.56, 28.22, 25.36, 25.13, 17.15. $C_{26}H_{26}N_2O_2$ (398.50): calcd. C 78.36, H 6.58, N 7.03; found C 78.41, H 6.36, N 7.24.

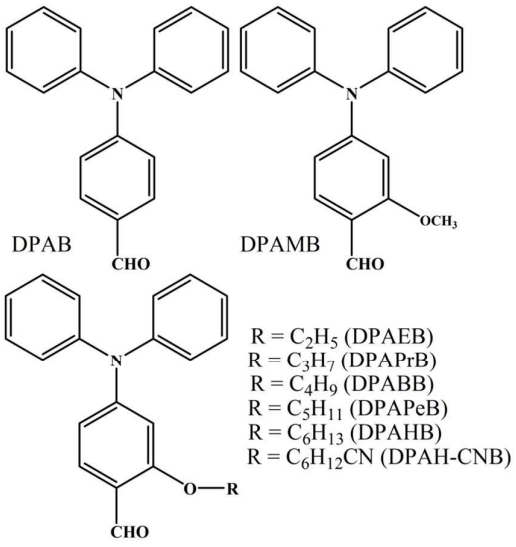

Scheme 1. Molecular structure of alkyl substituted compound.

Characterization

Absorption and fluorescence spectra were recorded using Perking Elmer 1050 and Jasco fluorescence spectrometer-FP-8300 instruments. Powder X-ray diffraction (PXRD) patterns were measured using a XRD- Bruker D8 Advance XRD with Cu Kα radiation (λ = 1.54050 Å). Single crystals were coated with paratone-N oil and the diffraction data measured at 100K with synchrotron radiation (λ = 0.62998 Å) on a ADSC Quantum-210 detector at 2D SMC with a silicon (111) double crystal monochromator (DCM) at the Pohang Accelerator Laboratory, Korea. CCDC Nos. – 1485284-1485289 and 1571829 contains the supplementary crystallographic data for this paper. Crystal structure of DPAB has already been reported (CCDC No. 676904).

Results and Discussion

The structures of different alkyl chain length substituted molecules are shown in Scheme 1. The absorption spectra of DPAB and different alkyl chain substituted compounds (DPAMB, DPAEB, DPAPrB, DPABB, DPAPeB, DPAHB and DPAH-CNB) in polar to non-polar solvent did not show significant change. All compounds showed λ_{max} between 351 to 362 nm, corresponding to intramolecular charge transfer (CT) transition (Fig. S1-2, Table S1). Similarly, the increase of alkyl chain length also did not influence significantly on the absorption (Table S1). The small absorption changes of DPAB and alkyl substituted compounds across polar to non-polar solvents suggest the slight dipolar alteration or negligible electronic intermolecular interaction in the ground state. In contrast, all compounds showed remarkable solvatochromic shift of fluorescence λ_{max} (77 nm shift) with different solvent polarity (Fig. 1, S3-4, Table S1. DPAB showed strong fluorescence at 452 nm in toluene, 509 nm in CH_2Cl_2, very weak fluorescence at 529 nm in polar CH_3CN and DMSO and no measurable fluorescence in CH_3OH. Different alkyl chain substituted compounds (DPAMB, DPAEB, DPAPrB, DPABB, DPAPeB, DPAHB and DPAH-CNB) also exhibited similar fluorescence shift in different polar solvents. The small absorption changes and strong red shift of fluorescence in different polar solvents suggest that DPAB and alkyl chain substituted compounds formed TICT (twisted intramolecular charge transfer) state in solvents.[14] The formation of polar excited state of DPAB and alkyl chain substituted compounds were more easily influenced by the solution polarity.[15] The influence of solvent polarity with the polar excited state (TICT) of DPAB and alkyl chain substituted compounds lead to the tunable fluorescence from 452 nm to 529 nm. The temperature dependent fluorescence change in solution and solvent polarity dependent fluorescence tuning further confirmed the formation of TICT state (Fig. S5-6).[16] Similar absorption and fluorescence of DPAB and alkyl chain substituted compounds indicate that alkyl chain length had negligible influence on the absorption and fluorescence properties in solution state.

Single crystals of DPAB, DPAMB, DPAEB, DPAPrB, DPABB, DPAPeB, DPAHB and DPAH-CNB were grown from ethanol /hexane and structural analysis were performed to get the

View Article Online
DOI: 10.1039/C7CE01650F

insight on the effect of alkyl chain length on the molecular packing in the solid state. H-bonding interaction between

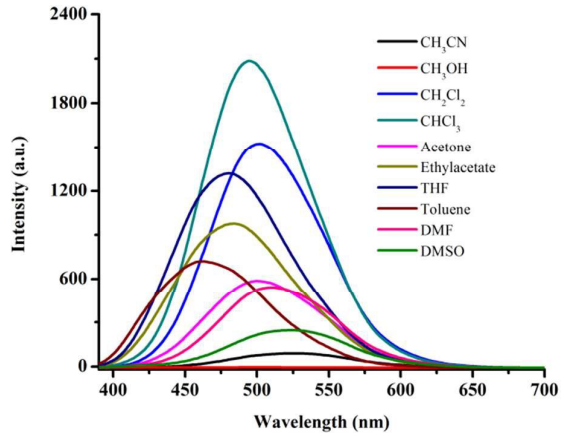

Fig. 1. Fluorescence spectra DPAPeB in different solvents.

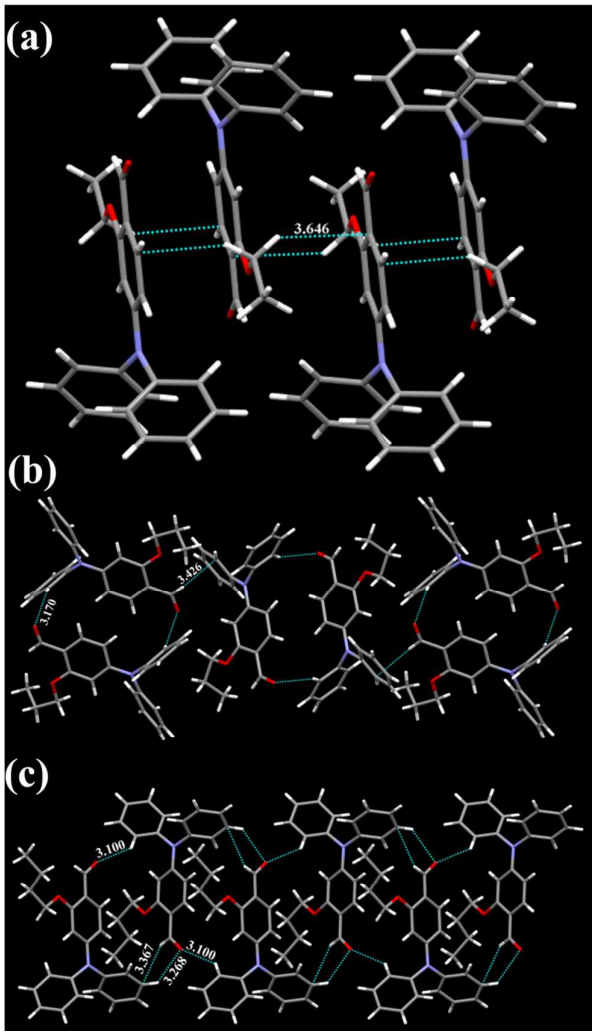

Fig. 2. Weak intermolecular interactions in the crystal lattice of (a) DPAB and (b) DPAMB. C (grey), N (blue), O (red), H (white). H-bonding and C-H…π interactions (broken line) distances are marked in Å.

aldehyde oxygen and phenyl hydrogen atoms resulted in the formation of dimer with opposite molecular orientation and 1-D network structure in DPAB crystal lattice (Fig. 2a). In DPAMB, H-bonding interactions between aldehyde oxygen and phenyl hydrogen leads to oppositely arranged molecular dimer (Fig. 2b, S7a). The dimers are further linked by H-bonding interactions between aldehyde oxygen and phenyl hydrogen of another DPAMB and C-H…π interactions that produced 2-D structure in the crystal lattice (Fig. 2b). Interestingly, aldehyde oxygen of DPAEB did not show any H-bonding interactions rather methylene group of ethyl alkyl chain formed C-H…π

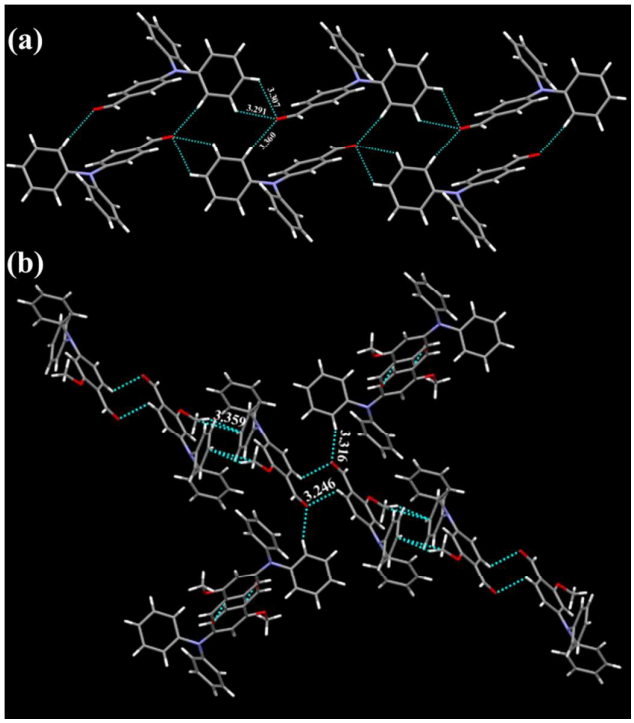

Fig. 3. Weak intermolecular interactions in the crystal lattice of (a) DPAEB, (b) DPAPrB and (b) DPABB. C (grey), N (blue), O (red), H (white). H-bonding and C-H…π interactions (broken line) distances are marked in Å.

interaction with aldehyde attached aromatic ring and produced dimer structure with opposite molecular orientation (Fig. 3a, S1b). However, DPAPrB exhibited dimer in the crystal lattice through H-bonding interactions between aldehyde oxygen and phenyl hydrogen and C-H…π interactions interlinked the dimers (Fig. 3b, S1c). Similarly, H-bonding interactions between aldehyde oxygen and phenyl hydrogen in both DPABB and DPAPeB produced dimer as well as network structure with opposite molecular orientation in the crystal lattices (Fig. 3c, 4a, S8). DPAHB did not show any intermolecular interactions in the crystal lattice and the molecules are well separated by hexyl alkyl chain (Fig. 4b, S8). In contrast, DPAH-CNB showed dimer structure via H-bonding interactions between aldehyde oxygen and phenyl hydrogen Fig. 4c, S9). The dimers were inter-linked through intermolecular interactions between cyano alkyl chain and phenyl group of adjacent dimer (H-bonding interactions

View Article Online
DOI: 10.1039/C7CE01650F

between cyano nitrogen and phenyl hydrogen and C-H…π interaction). The molecular packing of DPAB, DPAMB, DPAEB,

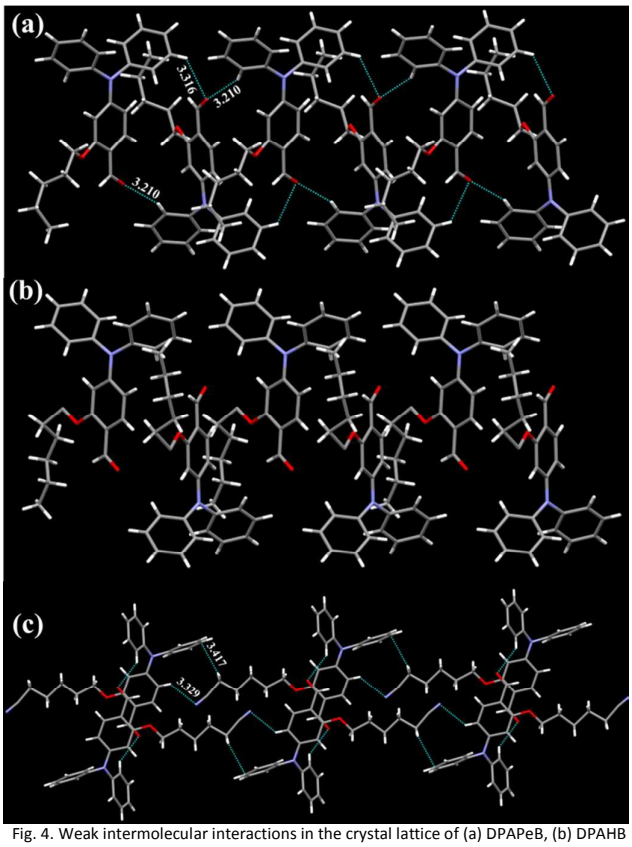

Fig. 4. Weak intermolecular interactions in the crystal lattice of (a) DPAPeB, (b) DPAHB and (b) DPAH-CNB. C (grey), N (blue), O (red), H (white). H-bonding and C-H…π interactions (broken line) distances are marked in Å.

DPAPrB, DPABB, DPAPeB, DPAHB and DPAH-CNB revealed that increase of alkyl chain lead to surfactant assembly of alkyl chains in the crystal lattice (Fig. S7-S9). In DPAMB and DPAEB, alkyl group in adjacent molecules are well separated but oriented in opposite direction. However, further increase of alkyl chain length lead to clear surfactant assembly in the crystal lattice. DPABB, DPAPeB and DPAHB showed similar molecular packing and alkyl group assembly in the crystal lattice. The butyl, pentyl and hexyl alkyl chains separate the dimers in the crystal lattice along *ac* plane. DPAH-CNB, cyano attached hexyl alkyl chain substituted, also produced similar surfactant assembly of alkyl chains and separation of dimers in the *bc* plane. Thus the molecular packing revealed that increase of alkyl chain length in DPAB produced surfactant assembly and well separation of dimers in the crystal lattice. The superimposed image of all structures revealed different conformational twist in the TPA phenyl rings depend on alkyl chain substitution (Fig. 5). Alkyl chain in all structures showed nearly similar bending conformation/orientation except hexyl cyano alkyl chain that showed straighter orientation due to H-bonding formation.

Contrast to the solution state, the slight conformational and packing differences in the solid state lead to tunable fluorescence from 429 to 490 nm. DPAB crystalline materials showed strong fluorescence at 448 nm (Fig. 6a). The crystals of

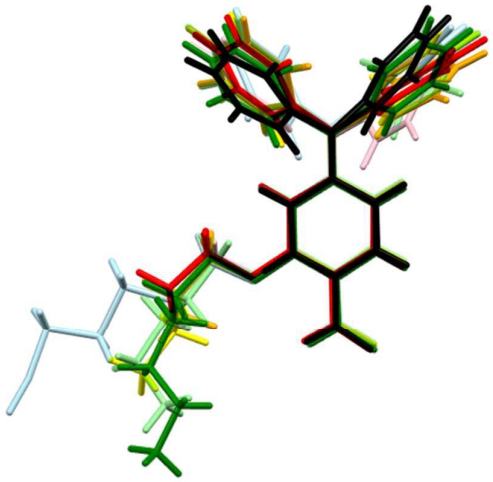

Fig. 5. Super-imposed structure of DPAB and alkyl chain substituted compounds. DPAB (black), DPAMB (blue), DPAEB (red), DPAPrB (white), DPABB (blue), DPAPeB (red), DPAHB (white) and DPAH-CNB (white).

DPAMB, DPAEB, DPAPrB, DPABB, DPAPeB, DPAHB and DPAH-CNB showed very weak/no fluorescence but hard crushing exhibited strong increase of fluorescence intensity without significantly shifting λ_{max}. (Fig. 6b, 7, S10-11). Hard crushing of DPAB slightly reduced the fluorescence intensity without altering the λ_{max}. DPAMB crystals showed very weak fluorescence at 452 nm that was significantly enhanced upon hard crushing (Fig. 6b). Surprisingly, DPAEB crystals as well as hard crushed sample did not show any strong fluorescence (Fig. 10a). DPAPrB, DPABB and DPAPeB crystals that showed very weak fluorescence showed strongly enhanced fluorescence at 442, 448 and 446 nm, respectively after hard crushing (Fig. S10b, 11). DPAHB crystals showed weak and strong fluorescence at 429 nm before and after hard crushing (Fig. 7a). DPAH-CNB, cyano group attachment at the end of hexyl chain, showed red shifted weak fluorescence, λ_{max} at 490 nm (Fig. 7b). Hard crushing strongly enhanced the fluorescence intensity with slight blue shift of λ_{max} (464 nm). Interestingly, melting of DPAB, DPAMB, DPAEB, DPAPrB, DPABB, DPAPeB, DPAHB and DPAH-CNB produced red shifted fluorescence (Fig. 6-7, S10-11). The melt of DPAB and DPAMB showed fluorescence at 475 and 466 nm, respectively. DPAEB melt exhibited fluorescence at 490 nm whereas DPAPrB, DPABB, DPAPeB and DPAHB melt showed florescence at 461 nm. The cyano substituted DPAH-CNB melt showed red shifted fluorescence at 480 nm. The slight rubbing of the melt showed reversible fluorescence switching (Fig. 6-7, S10-11). DPAB and DPAMB melt showed blue shifting of fluorescence to 451 nm upon slight rubbing (Fig. 6. The slight rubbing of DPAEB melt leads to blue shift of fluorescence with substantial decrease of intensity (Fig. S9a). DPAPrB, DPABB and DPAPeB melt showed fluorescence at 443, 448 and 446 nm after slight rubbing (Fig. S10b, S11). DPAHB melt showed fluorescence at 432 nm after slight rubbing melt and DPAH-CNB melt fluorescence was blue

View Article Online
DOI: 10.1039/C7CE01650F

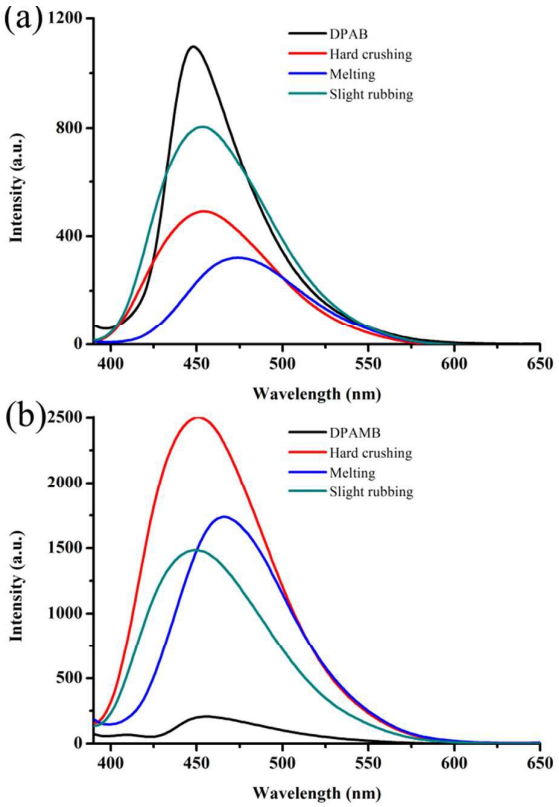

Fig. 6. Solid state fluorescence spectra (a) DPAB and (b) DPAMB (λ_{exc} = 360 nm).

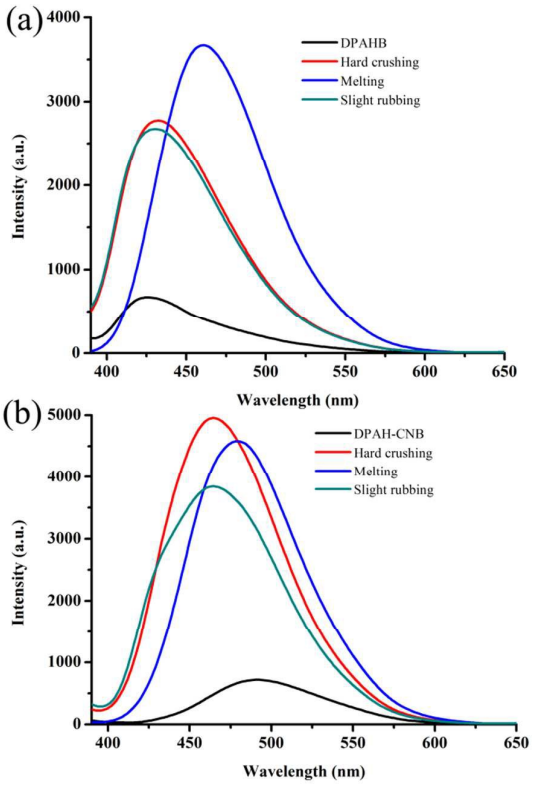

Fig. 7. Solid state fluorescence spectra (a) DPAHB and (b) DPAH-CNB (λ_{exc} = 360 nm).

shifted to 464 nm upon slight rubbing (Fig. 7). The reversible fluorescence switching via melting and rubbing can be performed for several cycles without significant change of fluorescence λ_{max}. The crystallization induced fluorescence switching can also be utilized for information writing on a glass plate (Fig. 8). PXRD studies indicate that crystalline solid was converted to amorphous phase while melting whereas slight rubbing regenerates the crystallinity in the sample (Fig. 9, S12-13). Hence, the conversion of crystalline (ordered state) to amorphous (disordered state) and amorphous (disordered state) to crystalline phase (ordered state) was responsible for exhibiting reversible fluorescence switching.

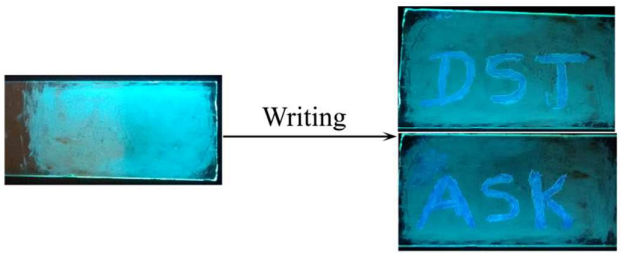

Fig. 8. Information writing on a glass plate using melt of DPAPeB.

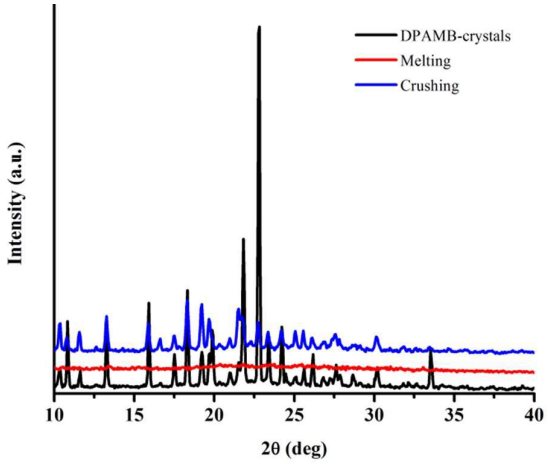

Fig. 9. PXRD pattern of DPAMB.

Importantly, DPAB, DPAMB, DPAEB, DPAPrB, DPABB, DPAPeB, DPAHB and DPAH-CNB exhibited alkyl chain length dependent self-reversible or stable blue fluorescent liquid after melting. Interestingly, DSC studies of DPAB, DPAMB, DPAEM, DPAPrB, DPABB, DPAPeB, DPAHB and DPAH-CNB revealed alkyl chain dependent crystallization/stable super cooled fluorescent liquid upon heating and cooling cycles (Fig. 10, S14-16).[11] DSC of DPAB showed melting point at 134 °C in the first heating and cooling did not show any changes (Fig. S14a). It is noted that molten organic crystalline materials may remain as supercooled liquid state due to the restricted molecular motion at low temperature and retardation of crystal growth. However, the subsequent heating of molten state could induce crystallization. Similarly, the second heating of DPAB showed a clear crystallization point at 58 °C before

View Article Online
DOI: 10.1039/C7CE01650F

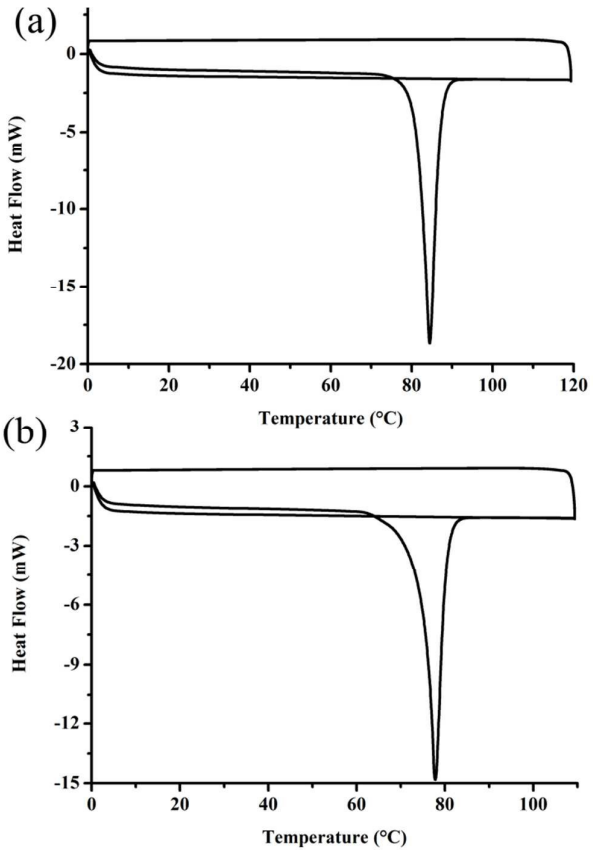

Fig. 10. Heating, cooling, heating and cooling DSC cycle of (a) DPABB and (DPAH-CNB).

melting at same temperature. The first heating of DPAMB also exhibited melting point at 134 °C and cooling did not show any significant changes (Fig. S14b). But the second heating showed a clear crystallization hump at 107 °C before melting at same temperature. Interestingly, DPAEB showed two melting points at 113 and 118 °C (Fig. S15a). The cooling cycle showed two phase transformations at 72 °C and 47 °C and suggests the solidification of melt. The second heating cycle of DPAEB also showed similar two melting points at same temperature. At present, it is not clearly understood for this unusual behaviour of DPAEB. It is noted that DPAEB showed different fluorescence behaviour (quenching upon solidification) compared to other compounds (fluorescence switching) and also exhibited dimer formation differently compared to other compounds. Thus DPAB, DPAMB and DPAEB melted while heating and clear crystallization followed by melting in the second heating cycle. Interestingly, DPAPrB, DPABB, DPAPeB, DPAHB and DPAH-CNB showed only one melting point while heating and did not exhibit crystallization either in cooling as well as second heating cycle (Fig. S15b, 16). This clearly suggests that the increase of alkyl chain length retard crystallization and produce quite stable fluorescent liquid at low temperature. The digital fluorescent images of DPAB, DPAMB and DPAEB melt also supported the quick self-conversion of fluorescence (Fig. 11). DPAB and DPAMB that showed cyan fluorescent melt self-reversed to blue fluorescent solid within 2 h. The strongly fluorescent DPAEB melt was converted to non-fluorescent solid within 4 h. But DPAPrB, DPABB, DPAPeB, DPAHB and DPAH-CNB melt also exhibited slow self-reversing of fluorescence from melt at different rate depending on the alkyl chain length. DPAPrB melt was self-reversed from cyan to blue after one day at room temperature and suggest the conversion of melt to solid state. The cyan fluorescence of DPABB and DPAPeB melt was converted to blue after standing 36 h at room temperature. In contrast, DPAHB and DPAH-CNB melts cyan fluorescence was converted to blue after 48 h. In contrast, slight rubbing of melt that provides the nucleation to convert the melt to solid showed reversible fluorescence from cyan to blue immediately. Further, unlike most of the reported melt that showed no/weak fluorescence in the melt, DPAB, DPAMB, DPAEB, DPAPrB, DPABB, DPAPeB, DPAHB and DPAH-CNB melts showed strong fluorescence might be due to the propeller structure of triphenylamine. Hence, increase of alkyl chain length of triphenylamine fluorophore might produce supercooled fluorescent liquid with strong fluorescence.

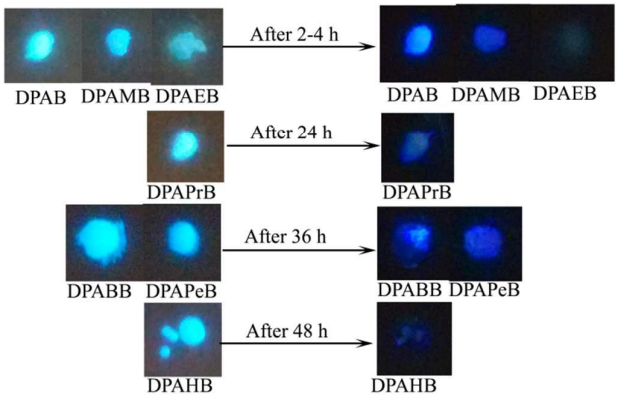

Fig. 11. Solid state fluorescence of melt-solid transition with time (λ_{exc} = 360 nm).

Conclusion

In conclusion, we have demonstrated crystallization induced reversible fluorescence switching and stable supercooled fluorescent liquid based on triphenylamine fluorophore by engineering alkyl chain length. The increase of alkyl length in DPAB leads to the formation lamellar arrangement in the solid structure. The change of alkyl chain length induced subtle conformational change on the TPA phenyl group that lead to tunable solid state fluorescence between 429 and 490 nm. All compounds showed strong fluorescence with red shifting of λ_{max} at molten state. The slight rubbing of the melt induced the crystallization and switch the fluorescence. PXRD studies confirmed the formation of amorphous phase in the melt and reversible conversion of amorphous to crystalline upon slight rubbing. Interestingly, the melt displayed alkyl chain length dependent stable fluorescent liquid formation. DPAB, DPAMB and DPAEB melt self-reversed to initial state within 2-4 h. DPAPrB melt was stable up to 24 h whereas DPABB and DPAPeB melt was stable up to 36 h. The fluorescent liquid of DPAHB and DPAH-

View Article Online
DOI: 10.1039/C7CE01650F

CNB was stable up to 48 h. Heating and cooling DSC cycles of DPAB and alkyl substituted compounds supported the alkyl chain dependent stable fluorescent liquid formation. Thus non-planar propeller shaped triphenylamine fluorophore could be employed for fabricating stable strongly fluorescent liquid by balancing the van der Waals and aromatic forces.

Acknowledgement

Financial support from the Science and Engineering Research Board (SERB), New Delhi, India (SERB No. EMR/2015/00-1891) is acknowledged with gratitude. The CRF facility of SASTRA University is also acknowledged for absorption spectroscopy. "X-ray crystallography at the PLS-II 2D-SMC beamline was supported in part by MSIP and POSTECH. DSC studies were supported by Basic Science Research Program through the National Research Foundation of Korea (NRF) funded by the Ministry of Education, Science and Technology (NRF-2017R1C1B2003111).

Notes and references

1 (a) S. J. Lim, B. K. An, S. D. Jung, M. A. Chung and S. Y. Park, *Angew. Chem., Int. Ed.,* 2004, **43**, 6346-6350; (b) S. P. Anthony, *ChemPlusChem*, 2012, **77**, 518-531; (c) S. Xu, H. Lu, X. Zheng and L. Chen, *J. Mater. Chem. C*, 2013, **1**, 4406-4422; (d) L. Xia, R. Xie, X. Ju, W. Wang, Q. Chen and L. Chu, *Nature Commun.,* 2013, **4**, 2226; (e) P. C. Xue, R. Lu, P. Zhang, J. Jia, Q. Xu, T. Zhang, M. Takafuji and H. Ihara, *Langmuir*, 2013, **29**, 417-425; (f) A. Pucci, F. D. Cuia, F. Signori and G. Ruggeri, *J. Mater. Chem.,* 2007, **17**, 783-790; (g) B. Xu, M. Xie, J. He, B. Xu, Z. Chi, W. Tian, L. Jiang, F. Zhao, S. Liu, Y. Zhang, Z. Xu and J. Xu, *Chem. Commun.,* 2013, **49**, 273-275; (h) S. Xu, H. Lu, X. Zheng and L. Chen, *J. Mater. Chem.* C, 2013, **1**, 4406.

2 (a) X. Zhang, Z. Chi, H. Li, B. Xu, X. Li, W. Zhou, S. Liu, Y. Zhang and J. R. Xu, *Chem.-Asian J.,* 2011, **6**, 808-811; (b) X. Zhang, Z. Chi, B. Xu, C. Chen, X. Zhou, Y. Zhang, S. Liu and J. Xu, *J. Mater. Chem.,* 2012, **22**, 18505-18513; (c) Q. Qi, X. Fang, Y. Liu, P. Zhou, Y. Zhang, B. B. Ang, W. Tian and S. X. Zhang, *RSC Adv.,* 2013, **3**, 16986-16989; (d) X. Y. Shen, Y. J. Wang, E. Zhao, W. Z. Yuan, Y. Liu, P. Lu, A. Qin, Y. Ma, J. Z. Sun and B. Z. Tang, *J. Phys. Chem. C,* 2013, **117**, 7334-7347; (e) S. P. Anthony, S. Varughese and S. M. Draper, *Chem. Commun.,* 2009, 7500-7502.

3 (a) Z. Chi, X. Zhang, B. Xu, X. Zhou, C. Ma, Y. Zhang, S. Liu and J. Xu, *Chem. Soc. Rev*., 2012, **41**, 3878–3896; (b) C. Feng, K. Wang, Y. Xu, L. Liu, B. Zou and P. Lu, *Chem. Commun.*, 2016, **52**, 3836-3839; (c) F. Zhang, Y. Hu, T. Schuettfort, C. Di, X. Gao, C. R. McNeill, L. Thomsen, S. C. B. Mannsfeld, W. Yuan, H. Sirringhaus, and D. Zhu, *J. Am. Chem. Soc.*, 2013, **135**, 2338–2345; (d P. S. Hariharan, D. Moon and S. P. Anthony, *J. Mater. Chem. C*, 2015, **3**, 8381-8388; (e) R. H. Pawle, T. E. Haas, P. Muller and S. W. Thomas, *Chem. Sci*., 2014, **5**, 4184.-4188.

4 (a) Y. Dong, B. Xu, J. Zhang, X. Tan, L. Wang, J. Chen, H. Lv, S. We, B. Li, L. Ye, B. Zou and W. Tian, *Angew. Chem. Int, Ed.,* 2012, **51**, 10782-10785; (b) Y. Wang, W. Liu, L. Bu, J. Li, M. Zheng, D. Zhang, M. Sun, Y. Tao, S. Xue and W. Yang, *J. Mater. Chem. C,* 2013, **1**, 856-862; (c) S. Yagai, T. Seki, T. Kitamura and F. Würthner, *Angew. Chem. Int. Ed.,* 2008, **47**, 3367-3371; (d) G. Zhang, J. Lu, M. Sabat and C. L. Fraser, *J. Am. Chem. Soc.* 2010, **132**, 2160–2162; (e) P. S. Hariharan, N. S. Venkataramanan, D. Moon and S. P. Anthony, *J. Phys. Chem. C*, 2015, **119**, 9460-9469; (f) A. Kundu, P. S. Hariharan, K. Prabakaran, D. Moon and S. P. Anthony, *RSC Adv.*, 2015, **5**, 98618-98625.

5 (a) T. Mutai, H. Satou and K. Araki, *Nat. Mater*. 2005, **4**, 685-687. (b) T. Mutai, H. Tomoda, T. Ohkawa, Y. Yabe and K. Araki, *Angew. Chem. Int. Ed.*, 2008, **47**, 9522 –9524. (c) Y. Zhao, H. Gao, Y. Fan, T. Zhou, Z. Su, Y. Liu and Y. Wang, *Adv. Mater.*, 2009, **21**, 3165–3169.

6 (a) H. V. Huynh, X. He and T. Baumgartner, *Chem. Commun.*, 2013, **49**, 4899-4901; (b) Y. I. Park, O. Postupna, A. Zhugayevych, H. Shin, Y.-S. Park, B. Kim, H.-J. Yen, P. Cheruku, J. S. Martinez, J. W. Park, S. Tretiak and H. -L. Wang, *Chem. Sci.,* 2015, **6**, 789-797; (c) K. -I. Sakai, S. Tsuchiya, T. Kikuchi and T. Akutagawa, *J. Mater. Chem. C.,* 2016, **4**, 2011-2016; (d) J. Li, B. Lv, D. Yan, S. Yan, M. Wei and M. Yin, *Adv. Funct. Mater.*, 2015, **25**, 7442-7449; (e) P. S. Hariharan, J. Pitchaimani, V. Muthu and S. P. Anthony, *Optical Materials,* 2017, **64**, 53-57; (f) P. S. Hariharan, E. M. Mothi, D. Moon and S. P. Anthony, *ACS Appl. Mater. Interfaces*, 2016, **8**, 33034-33042.

7 (a) S. Xue, X. Qiu, Q. Sun and W. Yang, *J. Mater. Chem. C.*, 2016, **4**, 1568-1578; (b) J. Mei and Z. Bo, *Chem. Mater.,* 2014, **26**, 604-615; (c) F. Zhang, Y. Hu, T. Schuettfort, C. Di, X. Gao, C. R. McNeill, L. Thomsen, S. C. B. Mannsfeld, W. Yuan, H. Sirringhaus and D. Zhu, *J. Am. Chem. Soc.*, 2013, **135**, 2338-2349; (d) X. Y. Wang, F. D. Zhuang, X. Zhou, D. C. Yang, J. Y. Wang, and J. Pei, *J. Mater. Chem.C,* 2014, **2**, 8152-8161; (e) J. Y. Back, T. K. An, Y. R. Cheon, H. Cha, J. Jang, Y. Kim, Y. Baek, D. S. Chung, S. K. Kwon, C. E. Park and Y. H. Kim, *ACS Appl. Mater. Interfaces.* 2015, **7**, 351-358; (f) Y. Wang, W. Liu, L. Bu, J. Li, M. Zheng, D. Zhang, M. Sun, Y. Tao, S. Xue and W. Yang, *J. Mater. Chem. C,* 2013, **1**, 856-862; (g) S. Kumar, P. Singh, R. Srivastava, R. R. Koner, A. Pramanik, J. Mathew, S. Sinha, M. Rawat, R. S. Anand and S. Ghosh, *J. Mater. Chem. C.* 2014, **2**, 6637-6647.

8 (a) S. Varghese and S. Das, *J. Phys. Chem. Lett*., 2011, **2**, 863-873; (b) S. Y. Yoon, J. W. Chung, J. Gierschner, K. S. Kim, M. G. Choi, D. Kim and S. Y. Park, *J. Am. Chem. Soc.*, 2010, **132**, 13675-13683; (c) M. Martinez-Abadi, S. Varghese, R. Gimenez and M. B. Ros, *J. Mater. Chem. C.*, 2016, **4**, 2886-2893; (d) N. D. Nguyen, G. Q. Zhang, J. W. Lu, A. E. Sherman and C. L. Fraser, *J. Mater. Chem.*, 2011, **21**, 8409-8415; (e) G. Q. Zhang, J. P. Singer, S. E. Kooi, R. E. Evans, E. L. Thomas and C. L. Fraser, *J. Mater. Chem.,* 2011, **21**, 8295-8299; (f) M. Sase, S. Yamaguchi, Y. Sagara, I. Yoshikawa, T. Mutai and K. Araki, *J. Mater. Chem.*, 2011, **21**, 8347-8354; (g) Y. Sagara, T. Mutai, I. Yoshikawa and K. Araki, *J. Am. Chem. Soc.*, 2007, **129**, 1520-1521; (h) P. S. Hariharan, P. Gayathri, D. Moon and S. P. Anthony, *ChemistrySelect*, 2017, **2**, 779-7807.

9 P. Srujana and T. P. Radhakrishnan, *Angew. Chem. Int. Ed.*, 2015, **54**, 7270–7274.

10 M. S. Yuan, D. E. Wang, P. Xue, W. Wang, J. C. Wang, Q. Tu, Z. Liu, Y. Liu, Y. Zhang and J. Wang, *Chem. Mater.*, 2014, **26**, 2467-2477.

11 K. Chung, M. S. Kwon, B. M. Leung, A. G. Wong-Foy, M. S. Kim, J. Kim, S. Takayama, J. Gierschner, A. J. Matzger and J. Kim, *ACS Cent. Sci.*, 2015, **1**, 94–102.

12 Y. Li, L. Xue, H. Xia, B. Xu, S. Wen and W. Tian, *J. of Polymer Sci: Part A: Polymer Chem.* 2008, **46**, 3970-3984.

13 A. Matoliukstyte, J. V. Grazulevicius and V. Jankauskas, *Mol. Cryst. Liq. Cryst*., 2007, **466**, 85-100.

14 (a) C. Cao, X. G. Liu, Q. Qiao, M. Zhao, W. Yin, D. Mao, H. Zhang, Z. C. Xu, *Chem. Commun.,* 2014, **50**, 15811–15814; (b) Z. R. Grabowski and K. Rotkiewicz, *Chem. Rev.,* 2003, **103**, 3899-4032.

15 (a) Y. Pan, J. Huang, W. Li, Y. Gao, Z. Wang, D. Yu, B. Yang and Y. Ma, *RSC Adv.*, 2017, **7**, 19576; (b) C. Reichardt, *Chem. Rev.*, 1994, **94**, 2319.

View Article Online
DOI: 10.1039/C7CE01650F

16 (a) R. Hu, E. Lager, A. Aguilar-Aguilar, J. Liu, J. W. Y. Lam, H. H. Y. Sung, I. D. Williams, Y. Zhong, K. S. Wong, E. Peña-Cabrera and B. Z. Tang, *J. Phys. Chem. C* 2009, **113**, 15845–15853; (b) X. Chen, X. Zhang and G. Zhang, *Chem. Commun.*, **2015**, ***51***, 161—163.

View Article Online
DOI: 10.1039/C7CE01650F

Graphical Abstract

Crystallization induced reversible fluorescence switching and alkyl chain length dependent thermally stable supercooled organic fluorescent liquid

Triphenylamine fluorophore produced alkyl chain length dependent stable fluorescent liquid and crystallization induced reversible fluorescence switching.